

Destructive inspection of Weld Defect and its Nondestructive Evaluation by Photoacoustic Microscopy

溶接欠陥の破壊検査および光音響顕微鏡による非破壊評価

Daijiroh Shiraishi[†], Ryosuke Kato, Haruo Endoh and Tsutomu Hoshimiya (Facult. Eng., Tohoku Gakuin Univ.)

白石大二郎, 加藤量介, 遠藤春男, 星宮 務 (東北学院大 工)

1. Introduction

At present, the welding is the key technology used in fabricating many structural components. However, welding might arise various inside defects in the juncture in the case when the welding is carried out with careless operation. The photoacoustic microscope (PAM)¹⁻³⁾ has been revealed effective tool for the nondestructive detection of the surface, internal and through defects, in which the detection is difficult with the conventional inspection method.

In this study, the welded specimen was fractured by forced bending in order to measure the defect size and shape directly which exists in the welded specimen. The stereoscopic image of the fractured specimen obtained by the destructive inspection was compared with the obtained photoacoustic (PA) amplitude image.

2. Experimental Apparatus and Specimen

The basic arrangement of the PAM system constructed for this experiment is the same as that described in a previous publication.²⁾ The specimens used in the experiments were aluminum plates. The aluminum specimen sampled from welded plates was chosen to include the weld defect. Two 45 degree-cut aluminum plates with the dimension of 25 mm×40 mm and a thickness of 4 mm were welded along y-direction as shown in Fig. 1. The welded specimen was compulsorily fractured and the scanning laser microscope (SLM) was used for the measurement of the fractured specimen surface.

3. Experimental Result and Discussions

The conceptual view of measurement direction by PAM and SLM is schematically illustrated in Fig. 2.

Fig. 3 shows the stereoscopic image of the fracture surface obtained by the SLM measurement

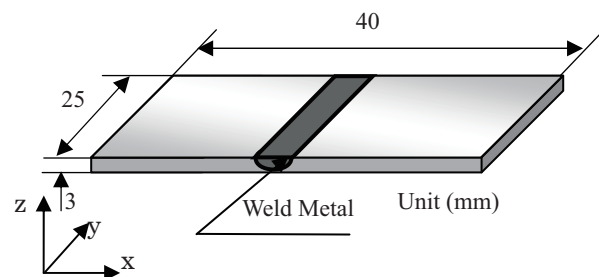


Fig. 1 Schematic drawing showing specimen preparation.

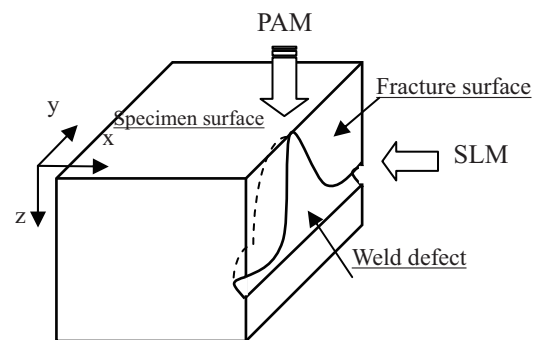


Fig.2 Conceptual view of measurement direction by PAM and SLM of specimen

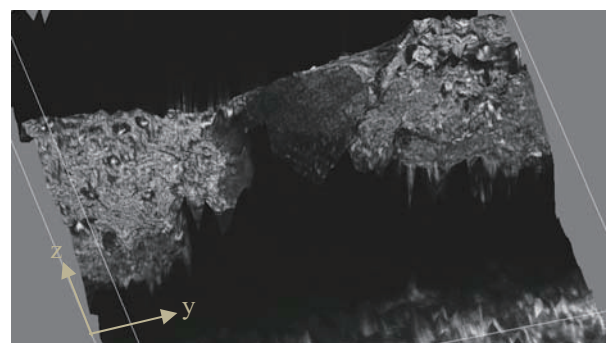


Fig. 3 SLM photograph of the fracture surface under the region including the weld defect. (Stereoscopic image)

of the central part of the region including the weld defect.

Fig. 4 is a composite SLM image of the entire

E-mail : enpal@tjcc.tohoku-gakuin.ac.jp

weld defect region, which was obtained by combining photographs of 5 times 4 image sheets.

The thermal diffusion lengths (λ) for PAM measurement at modulation frequencies of 12 Hz and 36 Hz were calculated to be 1550 μm and 895 μm , respectively. The distances measured from the specimen surface to the lines a-a' and b-b' in Fig. 4 was adjusted to be the thermal diffusion length of modulation frequencies of 12 Hz and 36 Hz, respectively.

In Fig.4, the line a-a' is located nearly at the bottom of the weld defect, and the size of the weld defect is about 4630 μm . In addition, the size of the weld defect is at line b-b' is approximately 1860 μm .

The specimen of PAM measurement was composed of the fractured specimens butted at the fracture surface, which were set in a PA sell. The experiments were carried out at different modulation frequencies to obtain the depth profiling by changing the thermal diffusion length.

Fig. 5(a) shows the amplitude image obtained at the modulation frequency of 12 Hz for the specimen for the weld defect and the measured area was 5.0 mm \times 5.0 mm. A bright area at the center of the PA amplitude image in Fig. 5(a) corresponds to the weld defect. From this PA image, it is found that dimensions of the weld defect are length (y-direction) of about 4600 μm and maximum width (x-direction) of about 2000 μm . In addition, from the SLM analysis result, the length (y-direction) of the weld defect is measured with about 4630 μm from the a-a' line in Fig 4. From this fact, it is found that defect length obtained from the PAM image and that obtained from the SLM are approximately same dimensions. Fig. 5(b) is the signal intensity distributions along the A-A' line of the PA amplitude image in Fig. 5(a). The size of the weld defect is measurable again from the signal strength distribution. Furthermore, it is proven that Fig. 5(a) also shows the weld defect inside (x-direction) which cannot be measured with the SLM.

Fig. 6(a) shows the PA amplitude image obtained at the modulation frequency of 36 Hz for the same specimen for the weld defect. Fig. 6(b) shows the signal intensity distribution on the B-B' line of the PA amplitude image in Fig. 6(a). From the PA amplitude image in Fig. 6(a) and Fig. 4, the length (y-direction) of the weld defect was measured with approximately 2100 μm and 1860 μm , respectively.

4. Conclusion

By accomplishing the destructive test for the measurement of welding internal defect in welded specimen, both the direct measurement of the weld

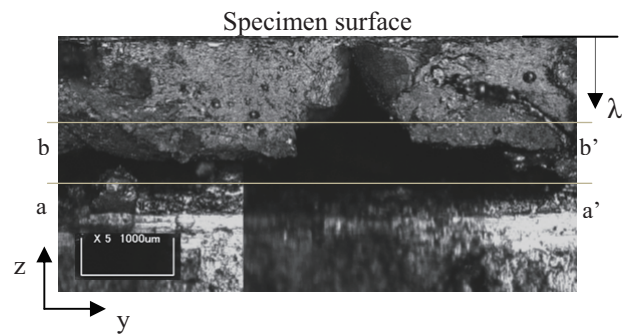
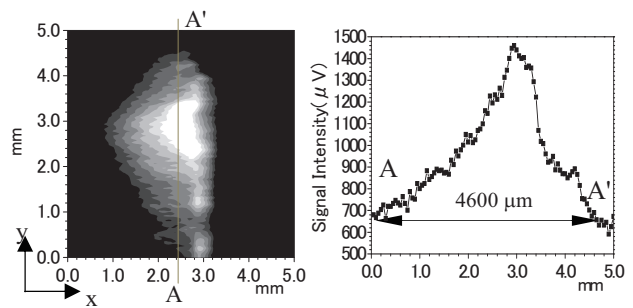


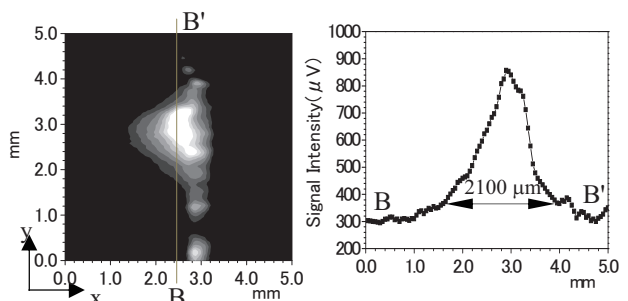
Fig. 4 SLM photograph of the entire image of the weld defect



(a) Amplitude image

(b) Signal distribution line A-A'

Fig. 5 PA amplitude image and signal distribution for the specimen with weld defect (modulation frequencies: 12Hz)



(a) Amplitude image

(b) Signal distribution line B-B'

Fig. 6 PA amplitude image and signal distribution for the specimen with weld defect (modulation frequencies: 36Hz)

defect from fracture surface and nondestructive measurement by PAM were performed. As a result, the size of the weld defect measured by each method was an about same dimension.

References

1. T. Hoshimiya, H. Endoh and Y. Hiwatashi: Jpn. J. Appl. Phys. **34** (1996) 3474.
2. H. Endoh, Naoki Ohtaki and T. Hoshimiya,: Jpn. J. Appl. Phys. **45** (2006) 4609.
3. T. Hoshimiya and K. Miyamoto: Jpn. J. Appl. Phys. **39** (2000) 3172.